Electron-scattering cross sections and stopping powers in H_2O

A. Muñoz,[1] J. C. Oller,[1] F. Blanco,[2] J. D. Gorfinkiel,[3] P. Limão-Vieira,[4] and G. García[5]
[1]*Centro de Investigaciones Energéticas, Medioambientales y Tecnológicas (CIEMAT), Avenida Complutense 22, 28040 Madrid, Spain*
[2]*Departamento de Física Atómica, Molecular y Nuclear, Universidad Complutense de Madrid, Avenida Complutense s.n., 28040 Madrid, Spain*
[3]*Department of Physics and Astronomy, The Open University, Walton Hall, Milton Keynes MK7 6AA, United Kingdom*
[4]*Departamento de Física, Universidade Nova de Lisboa, 2829-516 Caparica, Portugal*
[5]*Instituto de Matemáticas y Física Fundamental, Consejo Superior de Investigaciones Científicas (CSIC), Serrano 113-bis, 28006 Madrid, Spain*

(Received 10 July 2007; published 19 November 2007; corrected 10 December 2007)

Total electron-H_2O scattering cross sections have been measured from 50 to 5000 eV with experimental errors of about 5%. Integral elastic and inelastic cross sections have been calculated over a broad energy range (1–10 000 eV) with an optical potential method assuming an independent atom representation. Dipole rotational excitations have also been included in the framework of the first Born approximation. From a detailed evaluation of the present results and their comparison with previous theoretical and experimental data, a set of recommended integral cross sectional data is provided. By combining these data with an average excitation energy derived from the experimental energy loss spectra, the stopping power of electrons in H_2O has been obtained from 5 to 5000 eV.

DOI: 10.1103/PhysRevA.76.052707 PACS number(s): 34.80.Bm, 34.80.Gs, 34.50.Bw

I. INTRODUCTION

In the past few years, radiation damage in biomolecular systems has been the subject of extensive research work. Recent studies show that secondary electron interactions with atoms and molecules constituting the medium are the main cause of this damage [1,2]. In addition, these studies are also relevant for some beneficial applications of radiation in medical diagnosis and radiotherapy. For these reasons, accurate radiation interaction models, that include secondary electron effects, require electron scattering cross sections over a wide energy range, in principle, from the high energy of the primary particle slowing down to thermal energies. Although these parameters have been widely studied for different atomic and molecular targets [3–5], most of the work has been restricted to the low energy domain. From the experimental point of view electron scattering cross section data for energies above 500 eV are scarce. Concerning calculations, a complete scattering treatment is not affordable at these energies and some approximations are required. For high energies, it is customary to use the first Born approximation to calculate cross section data, both for elastic and inelastic scattering. However, we have shown [6–9] that this approximation overestimates cross section values for simple life relevant molecules such as N_2, O_2, CH_4, and CO_2 even at 5000 eV incident electron energy. At intermediate and high energies (50 to 5000 eV) optical potential calculations assuming an independent atom configuration, have proven to be a simple and powerful tool [10–12] applicable to different sized molecules, from diatomic molecules to complex biomolecules [13].

One of the most important molecules for biological systems is water. Consequently, electrons interacting with H_2O molecules have been studied, both theoretically and experimentally, by means of different techniques. Results from these studies can be found in recent reviews [14,15] where tables with recommended cross sections for most representative collision processes can also be found. A significant number of experiments and calculations were surveyed to get these cross section values. Discrepancies between these compiled data for such an essential parameter as the total electron scattering cross section are about a factor 2 for energies below 10 eV and reliable data for energies above 1000 eV are almost nonexistent. Not much better is the situation for the ionization cross sections where discrepancies of about 25% persist from threshold to 1000 eV and no recent measurements can be found in the literature for higher energies. Computational efforts made in the last few years to improve precision in particle track simulations could be in vain if the accuracy of the cross section data on which they are based is not improved.

In addition, an important parameter to evaluate radiation effects in medical and environmental applications is the electron stopping power (STP). Results for these parameters, calculated with the Born-Bethe procedure described in [16], can be found in the NIST databases [17]. We have recently shown [18], for methane based tissue equivalent materials, that STP values derived from a combination of the electron scattering cross sections with the experimental energy loss spectra showed important discrepancies with those of [17]. A similar study for H_2 [19] suggests that some of these discrepancies are caused by the experimental uncertainty related to inner shell excitation processes. It is worthy to achieve analogous results for H_2O, where these processes can be relevant for energies above 500 eV.

Motivated by the above considerations, in this paper we present total electron scattering cross section (TCS) measurements which were performed in a transmission-beam experiment for incident energies between 50 and 5000 eV as well as total ionization cross sections derived from the simultaneous measurement of electron and ion currents for those electron energies. Integral elastic and inelastic cross sections in the energy range 1–10 000 eV have been calculated with an optical potential method in the framework of an independent atom representation. Present results have been compared with available theoretical and experimental data to

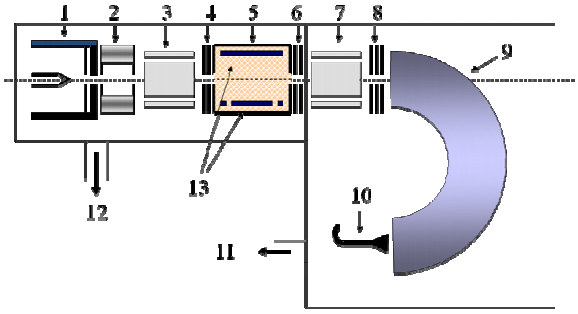

FIG. 1. (Color online) Experimental apparatus: 1, electron gun; 2, transverse magnetic field; 3, 7, quadrupole electrostatic plates; 4, 6, 8, decelerating and accelerating lenses; 5, scattering chamber; 9, hemispherical electrostatic energy analyzer; 10, channel electron multiplier; 11, 12 vacuum turbo pumps; 13 ion collecting plates.

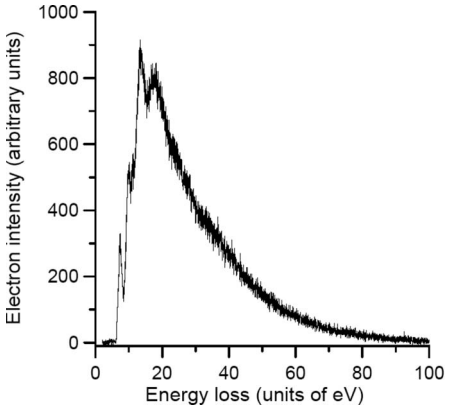

FIG. 2. Energy loss distribution function of electrons in water from 0 to 100 eV.

give a complete set of recommended integral electron scattering cross sections from 5 to 5000 eV. Following the procedure described in [19], these recommended values have been combined with the average excitation energies derived from our experimental energy loss spectra to obtain electron stopping powers in H_2O. The compatibility of this STP data with those of the NIST database will be discussed.

II. MEASUREMENTS

The experimental setup to measure TCS and energy loss spectra was based on that reported previously [20] including the recent improvements described in [21]. Here we will describe it briefly giving some details about the modification of the system required for a simultaneous measurement of electron and ion currents. A schematic of the apparatus is shown in Fig. 1. The primary beam was produced by an emitting filament. A combination of magnetic and electrostatic fields controls the direction of the beam and reduces the energy spread to 100 meV. The collision chamber containing the gas target was a stainless steel tube defined by two apertures. The entrance aperture was 0.5 mm in diameter. Different exit apertures with 1, 2, and 3 mm diameter as well as two different lengths of the collision chamber of 10 and 50 mm, respectively, were used according to the experimental requirements. The gas pressure in the chamber was measured with an absolute capacitance gauge (MKS Baratron 127A) and it was varied from 0.1 to 10 mTorr according to the experimental conditions. Electrons emerging from the collision chamber were deflected by a quadrupole electrostatic system to select the angle of analysis. The energy analyzer was a hemispherical electrostatic spectrometer in combination with a retarding field. In these conditions the energy resolution of the spectrometer was about 0.5 eV for the whole energy range considered here. Transmitted electrons through the analyzer were finally detected by a channel electron multiplier operating in single pulse counting mode. Counting rates were typically on the order of 10^3 s^{-1} for total cross section measurements and up to 10^4 s^{-1} through the energy loss spectra determination. The maximum angular acceptance of the energy analyzer was 1.9×10^{-5} s r.

To measure the ionization cross section, a parallel plate system was placed in the collision chamber. It consists of two circular copper plates of 30 mm diameter. One of them was equipped with a guard ring to ensure homogeneity of the electric field around the central ion collecting area of 10 mm diameter (see Fig. 1). In order to measure the average electron and ion currents, which were proportional to the actual current values, the electron beam was pulsed by applying a +10 V train of pulses to the gun control electrode, each of 10^{-5} s duration and having a repetition rate of 10^4 Hz. Extractive pulses of variable amplitude, up to +400 V, in synchronism with the electron beam pulses, were applied to the ion collecting plates. In these conditions, relative ionization cross section, as a function of the electron current, can be derived from the ratio ion/electron current for a given molecular density.

The whole system was differentially pumped by two turbo pumps of 70 and 250 l/s, respectively, reaching a background pressure of 10^{-8} Torr. The pressure in the electron gun and energy analyzer region was maintained lower than 10^{-6} Torr during the measurements.

TCS have been measured for energies between 50 and 5000 eV. Energy loss spectra were measured in the region 10–5000 eV at different scattering angles. These angles were selected by deflecting the scattered beam with a quadrupole electrostatic plate system. For each energy the mean excitation energy has been obtained by averaging energy loss spectra at different scattering angles. Since the intensity of the scattered signal decreases with the angle, the maximum scattering angle reached for a given energy was that for which the intensity of the inelastic peaks were less than the 10% of the corresponding intensity at 0°. This process ensures that the main contribution of the inelastic scattering, about 90%, has been included in our average procedure. A detail of the energy loss distribution function derived from the above procedure is shown in Fig. 2.

Relative ionization cross sections were measured from 50 to 5000 eV. Typical mean currents of the pulsed electron and ion beams were between 10^{-8} and 10^{-11} A, respectively, for gas pressures in the range $10^{-4}-10^{-3}$ Torr. These relative values were put on an absolute scale by normalizing to the electron impact ionization cross section for N_2 at 1000 eV which was assumed to be (3.05 ± 0.19) a_0^2 in accordance with previous measurements available in the literature [22–26].

III. CALCULATIONS

The optical potential method described in previous papers [10–12] has been used to calculate differential and integral elastic as well as integral inelastic electron-H_2O scattering cross sections. The calculation includes the recent adjustments we have introduced in the potential which significantly improved results for many molecular targets, both for integral [11] and differential [12] cross sections, especially in the low energy region. As this method considers the inelastic scattering as electron-electron interaction processes, only those arising from electronic excitation are considered, being rotational and vibrational excitations ignored. This restriction is not significant in general for the relatively high energies of our calculations but in the case of water, due to its permanent dipole moment, rotational excitation becomes more important than previously studied systems with this technique. To account for this, the procedure suggested in [27] was used. The method consists in the calculation of the rotational excitation cross section for a free electric dipole by assuming that the energy transferred is low enough, in comparison with the incident energy, to validate the first Born approximation (FBA). In these conditions, we have calculated an average rotational excitation cross section $J \rightarrow J'$ for water at 300 K by weighting the population of the J rotational quantum number at that temperature and assuming an average excitation energy. These rotational excitation cross sections can be added to the integral inelastic cross section.

Following the above procedures we present calculated integral electron scattering cross sections (elastic, inelastic, dipole rotational excitation, and total) from 1 to 10 000 eV. The reliability of these results will be discussed in the next section in comparison with the experimental data.

IV. RESULTS AND DISCUSSION

TCS measured in this study, from 50 to 5000 eV, are shown in Table I and plotted in Fig. 3. The estimated experimental errors of these data are less than 5% (see Ref. [20] for a detailed analysis of the main error sources). Representative previous measurements [28–36] are also included in this figure for comparison. As shown in this figure, there is a good agreement, within 10%, between present and previous experimental data from 50 to 1000 eV impact energies. Above this value, the only previous experimental data [31] diverge from those of the present work reaching discrepancies of about 30% at 3000 eV. The origin of this discrepancy has been widely discussed in preceding papers [37–39] and, as shown in Ref. [39], it is motivated by the poor energy and angular resolution used in Ref. [31]. Regarding theoretical data, Table I includes our calculated integral elastic, integral inelastic (absorption potential contribution), and dipole rotational excitation (from the FBA) cross sections. As may be seen in Fig. 3 total electron scattering obtained by adding those partial ones show an excellent agreement with our experimental data in the overlapping energy region (50–5000 eV). However, recent model potential calculations given in Ref. [40] deviate from ours for energies above 1000 eV following the aforementioned tendency of the experimental data of Ref. [31]. Considering that the accuracy of the model potential calculations should increase with energy, the origin of this behavior is not clear but its high energy tendency is shown in Fig. 4 and will be discussed later.

Going to the low energy region, important discrepancies between theory and experiment arise below 10 eV. While our approximate calculation agree reasonably with those given by the R-matrix method of Ref. [41] from 0.5 to 5 eV, early experiments give much lower values, a factor of 2 on average, in this energy range. As has been discussed by several authors [15,35], this discrepancy is motivated by the inability of these experiments to resolve dipole rotational excitations which are dominated for the $J=0 \rightarrow J=1$ transition of 4 meV excitation energy being electron scattered preferably in the forward direction. Kimura *et al.* [35] have recently corrected the measurements of Sueoka *et al.* [29] for this effect, as well as for other systematic errors, giving a complete set of data (see Fig. 3) that were considered by Itikawa and Mason [15] as recommended values for energies between 1 and 400 eV. However, a recent study of Čuric *et al.* [36] based on accurate transmission measurements leads to low energy total cross section values which are between the previous measurements and the calculated ones. This situation can be understood if we consider that, unlike preceding measurements, the 1.6 meV energy resolution used in [36] is good enough to resolve rotational molecular excitations and therefore the observed total cross section increases with respect to that of previous experiments. However, as measurements were carried out at room temperature, these excitations do not arise all from the lowest $J=0$ rotational state but from a distribution of different J up to $J=8$, leading to results lower than the calculations shown in Fig. 3, which consider all the excitations from the lowest rotational level. As a consequence, a direct comparison between theory and experiment at low energy is not possible unless we are considering the same initial conditions for the target: Cooling the target molecules to their ground rotational state in the experiments or considering an initial rotational population distribution in the calculations.

Turning to the high energy region, an important aspect is to compare the total cross section with those predicted by the first Born approximation and the Bethe theory [41–43]. It is customary to assume that these apply at high incident electron energies. However, as mentioned in the introduction section, we have found in previous studies [6–9] that these approximations overestimate the total cross section, and mainly the elastic part, for simple molecules as N_2, O_2, CH_4, and CO_2 even at 5000 eV. It is worth checking this point for the case of H_2O in order to look for the energy limit at which the Born approximation can be considered valid, thus providing a method to extrapolate cross section values at really high energies. Assuming an independent atom representation, total electron scattering from H_2O molecules can be derived from those of their constituent atoms. Using the Born-Bethe parameters for H and O calculated in Refs. [42–44], the following expression may be written:

TABLE I. Experimental and theoretical integral electron scattering cross sections obtained in this study.

	Calculation (a_0^2)				Experiment (a_0^2)	
Energy (eV)	Elastic (σ_{el})	Inelastic (σ_{inel})	Rotational (σ_r)	Total (σ_{tot})	Ionization (σ_{ion})	Total (σ_{tot})
1	107		356	463		
1.5	98.4		253	352		
2	90.4		199	289		
3	76.0		141	217		
4	64.2		110	174		
5	55.5		90.7	146		
7.5	47.1	0.001	63.8	111		
10	42.4	0.05	49.6	92.0		
15	35.7	1.77	34.7	72.2		
20	30.1	5.47	26.9	62.5		
30	22.2	11.4	18.7	52.3		
40	18.2	12.9	14.5	45.6		
50	15.6	13.1	11.9	40.6	6.65	36.6
75	11.9	12.4	8.24	32.5	7.95	30.7
100	9.77	11.4	6.35	27.5	8.26	26.4
150	7.42	9.73	4.40	21.5	7.72	21.2
200	6.11	8.50	2.39	18.0	6.93	17.9
300	4.65	6.84	2.34	13.8	5.74	14.1
400	3.83	5.75	1.80	11.4	4.88	11.6
500	3.28	5.00	1.46	9.74	4.29	9.66
750	2.45	3.78	1.01	7.24	3.16	7.09
1000	1.98	3.07	0.775	5.82	2.54	5.66
1500	1.44	2.25	0.533	4.22	1.83	4.12
2000	1.14	1.78	0.408	3.33	1.45	3.29
3000	0.814	1.26	0.280	2.35	1.05	2.41
4000	0.635	0.987	0.215	1.84	0.845	1.92
5000	0.523	0.811	0.174	1.51	0.702	1.60
7500	0.366	0.566	0.120	1.05		
10000	0.284	0.436	0.0914	0.811		

$$\sigma_T = \frac{1}{E}\left[1890 + 765.8\ln(E) - \frac{1}{E}38342\right], \qquad (1)$$

where σ_T is the total electron scattering cross section in a_0^2 units and E is the incident electron energy in eV. Figure 4 is a plot of $\sigma_T E$ as a function of $\ln(E)$ for data from Eq. (1) and for available theoretical and experimental values at energies above 1000 eV. As expected, data from Eq. (1) for increasing energies give a straight line which can be considered as the asymptotic behavior of the total cross sections. This behavior is followed both for our calculations and experimental data which tend to the Born-Bethe limit, being the difference only of 10% at 5000 eV. However, the experimental data of Ref. [31] and the calculations of [40], above 1000 eV, show a tendency divergent from the Born-Bethe limit.

Experimental ionization cross sections derived from this study are also shown in Table I and plotted in Fig. 3. Experimental errors, including the accuracy of the normalizing procedure, have been estimated at about 7%. As shown in Fig. 4 there is an excellent agreement, within 5%, with accurate measurements of Ref. [22]. However, recent calculations show important discrepancies with these experiments: values of Ref. [40] tend to be lower than the present ones reaching discrepancies of about 20% at 2000 eV while the distorted wave born approximation used in [45,46] are higher than the experimental ones with differences of about 30% for energies above 500 eV.

As mentioned in the Introduction section, reliable stopping power data for electrons in water are essential parameters in radiation based medical applications. The method we applied for other molecular targets has proven to give more accurate results than available databases [16,17], which are based on Born-Bethe calculations, when a consistent set of cross section data is accomplished. The set we are proposing for that purpose consists of the present experimental results

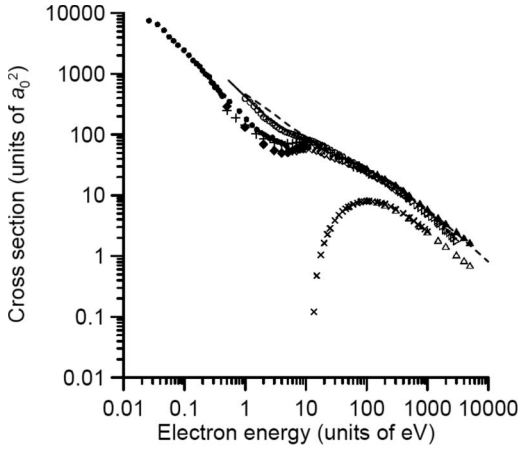

FIG. 3. Total electron scattering and ionization cross sections from H_2O. Present measurements: ▲, total scattering; △, ionization. Other measurements: ▷, [31]; ●, [36]; +, [30]; ○, [35]; ◇, [32]; ♦, [28]; ×, [22]. Calculations: - - -, present optical potential calculation; —, *R*-matrix calculation of [41].

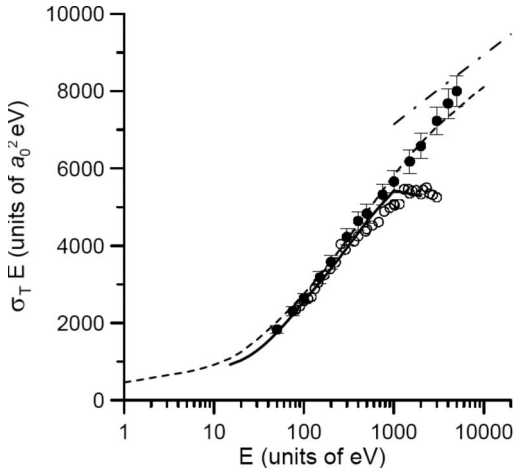

FIG. 4. Fano plot (total cross section multiplied by electron energy as a function of energy in a logarithmic scale): ●, present experimental data; ○, experimental data from [31]; - - -, present optical potential calculation; —, calculation of [40]; ··· Born-Bethe calculation.

from 50 to 5000 eV with error limits of ±5%. For lower energies, we propose an average of experimental data given in [30,35] to be used from 40 to 7.5 eV with statistical deviations between 5 and 18%, respectively. Below 7.5 eV experimental disagreements are larger than 20% and no experimental data can be recommended without specific considerations about the experimental conditions (temperature, energy distribution of incident electrons, scattering geometry). Finally, our calculations can be used to extrapolate data from 5000 eV to 10 000 eV. Above 10 000 eV, Eq. (1) provides reasonable TCS values. Estimated uncertainties of extrapolated data are about 10%. Recommended experimental data from 7.5 to 10 000 eV are shown in Table II. These values have been used to derive the collisional stopping power $(-dE/dx)_{\text{col}}$, or energy loss per unit path length (x), of electrons in H_2O according to the expression [19]

$$-\frac{1}{\rho}\left(\frac{dE}{dx}\right)_{\text{col}} = \frac{N_a}{M}\bar{E}\sigma_{\text{inel}}, \tag{2}$$

where ρ is the density of the target, σ_{inel} is the integral inelastic cross section, N_a is the Avogadro constant, M the molar mass, and $\bar{E}$ is a mean excitation energy that has been derived from the experimental energy loss spectra for incident energies ranging from 10 to 5000 eV. Rotational excitation has not been considered in this procedure as far as the transferred energy is of the order of a few meV which is negligible in comparison with the electronic excitation threshold, about 6.5 eV. Confirming this assumption, below 6.5 eV no inelastic signal was detected in our experimental energy loss spectra. Above this energy, mean excitation energies increase with incident energies up to 32±2 eV at 500 eV. Beyond the inner shell excitation threshold this values raise up to 40±2 eV remaining almost constant, within 10%, from 750 to 5000 eV incident energies.

Equation (2) can be expressed as a function of the total cross section by introducing a parameter $\gamma=\sigma_{\text{inel}}/\sigma_{\text{tot}}$ as follows:

$$-\frac{1}{\rho}\left(\frac{dE}{dx}\right)_{\text{col}} = \frac{N_a}{M}\bar{E}\gamma\sigma_{\text{tot}}. \tag{3}$$

The γ values derived from our optical potential calculation are shown in Table II.

Mass stopping powers obtained by introducing γ and σ_{tot} values of Table II in Eq. (3) are also shown in this table and plotted in Fig. 5 for comparison with previous data. By combining the uncertainty of magnitudes involved in Eq. (3), a total error of ±15% can be assigned to the present stopping power values. These parameters have been the subject of recent theoretical studies [47–51] in water, both for gas and liquid phase. From these references we can conclude that latest calculations present a general agreement as far as stopping power of electrons in water vapor is concerned, as well

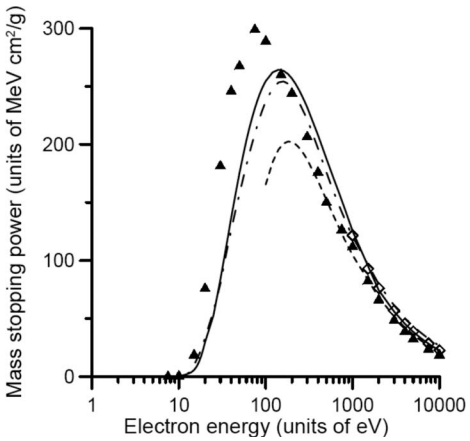

FIG. 5. Mass stopping power of electrons in H_2O. ▲, present results; ◇, values given in NIST database [17]; gas phase calculations: — [48], ··· [47]; liquid phase calculation: - - - [49,50].

TABLE II. Recommended total scattering cross sections, inelastic-total cross section ratio (γ), and mass stopping power for electrons in H_2O from 7.5 to 10000 eV.

			Mass stopping power (MeV cm^2/g)		
Energy (eV)	Total cross section (a_0^2)	Inelastic-total cross section ratio (γ)	This work	Ref. [48]	NIST [17]
7.5	84.0	0.00001	0.00497		
10	78.8	0.00054	0.3425	0.4584	
15	68.0	0.0245	18.53	5.845	
20	59.6	0.0876	75.84	29.75	
30	47.9	0.218	181.3	83.66	
40	41.4	0.283	245.8	136.5	
50	36.6	0.323	267.4	175.5	
75	30.7	0.381	298.9	231.3	
100	26.4	0.414	288.9	254.7	
150	21.2	0.451	260.1		
200	17.9	0.472	243.9	256.9	
300	14.1	0.494	206.4	232.0	
400	11.6	0.505	175.8	208.1	
500	9.66	0.513	149.8	187.7	
750	7.09	0.522	126.3		
1000	5.66	0.527	111.8	125.4	121.8
1500	4.12	0.532	82.26		93.12
2000	3.29	0.534	65.93	74.44	76.23
3000	2.41	0.535	48.33	56.18	56.89
4000	1.92	0.537	38.66	45.62	45.94
5000	1.60	0.537	32.23	38.66	38.82
7500	1.16	0.538	23.40		28.50
10000	0.92	0.537	18.52	22.65	22.70

as for the liquid phase, in the range 10–10 000 eV, converging to the NIST reference values [17] for energies above 10 keV. By introducing the present results in the discussion, Fig. 5 shows that our semiempirical stopping powers are in reasonable agreement, within the error limits, with previous calculations for energies ranging from 100 to 10 000 eV. However, below 100 eV while previous data tend to decrease present results continue increasing to reach a maximum value around 75 eV which is about 30% larger than those given in Refs. [48,49] for that energy. This tendency is even more prominent as compared with data corresponding to the liquid phase. Since this discrepancy could be originated in the relevance that our study gives to nonionizing inelastic excitations, differences with the liquid phase can be attributed to the strong dependence of these channels on the surrounding conditions of the molecule. However, at present no explanation has been found for discrepancies with the gas phase data. It seems that inelastic processes in previous studies are dominated by ionization which reaches maximum cross sections around 100 eV while nonionizing excitations have their maximum values at lower energies. Further experimental studies would be desirable to clarify this point.

V. CONCLUSIONS

In this study, we present accurate experimental cross sections for total electron scattering and total electron impact ionization from 50 to 5000 eV. These data are relevant parameters for radiation-based medical applications. Present results confirm that, in contrast with the behavior derived from previous high energy measurements [31] and calculations [40], integral electron scattering cross sections above 1000 eV tend to those predicted by the Born approximation, reaching a reasonable agreement at 10000 eV. Integral cross section data have also been calculated with an optical potential method over a broad energy range (1–10 000 eV) showing an excellent agreement with experiments above 10 eV.

From a comprehensive analysis of available experimental and theoretical data a set of recommended total scattering cross section from 10 to 10000 eV is provided. Below this energy we conclude that no recommendations can be given without additional considerations about the experimental conditions.

By combining the recommended cross section data with experimental energy loss spectra and calculated integral

cross sections we have derived semiempirical stopping powers of electrons in water vapor which agree with previous calculations for energies above 100 eV. For lower energies, discrepancies of about 30% have been found both in the position and the value of the maximum stopping power. No reason has been found when comparison is made between gas phase data. According to our model, subionizing inelastic channels have more weight than assumed in previous studies [48,49].

In spite of the great number of publications devoted to electron interactions in water, some aspects of the low energy electron scattering with water molecules remain unclear and further studies in this region will be desirable, particularly due to their relevance for living systems.

ACKNOWLEDGMENTS

This study has been partially supported by the following research projects and institutions: Ministerio de Educación y Ciencia (Plan Nacional de Física, Project FIS2006-00702), Consejo de Seguridad Nuclear (CSN), European Science Foundation (COST Action P9 and EIPAM Project), and Acciones Integradas Hispano-Portuguesas (Project HP2006-0042). We acknowledge N. C. Jones and D. Field for providing their unpublished cross section data.

[1] S. Gohlke, A. Rosa, E. Illemberger, F. Brüning, and M. A. Huels, J. Chem. Phys. **116**, 10164 (2002).
[2] X. Pan, P. Cloutier, D. Hunting, and L. Sanche, Phys. Rev. Lett. **90**, 208102 (2003).
[3] S. Trajmar, D. F. Register, and A. Chutjian, Phys. Rep. **97**, 219 (1983).
[4] M. J. Brunger and S. J. Buckman, Phys. Rep. **357**, 215 (2002).
[5] M. Jelisavcic, R. Panajotovic, and S. J. Buckman, Phys. Rev. Lett. **90**, 203201 (2003).
[6] G. García and F. Manero, Phys. Rev. A **53**, 250 (1996).
[7] G. García and F. Manero, Phys. Rev. A **57**, 1069 (1998).
[8] G. García and F. Blanco, Phys. Lett. A **279**, 61 (2001).
[9] G. García, F. Blanco, and A. Williart, Chem. Phys. Lett. **335**, 227 (2001).
[10] F. Blanco and G. García, Phys. Rev. A **67**, 022701 (2003).
[11] F. Blanco and G. García, Phys. Lett. A **317**, 458 (2003).
[12] F. Blanco and G. García, Phys. Lett. A **330**, 230 (2004).
[13] F. Blanco and G. García, Phys. Lett. A **360**, 707 (2007).
[14] *Photon and Electron Interactions with Atoms, Molecules and Ions*, Landolt-Börnstein, Group I, Vol. 17, Pt. A (Springer, Berlin/Heidelberg, 2003).
[15] Y. Itikawa and N. Mason, J. Phys. Chem. Ref. Data **34**, 1 (2005).
[16] International Commission on Radiation Units and Measurements, ICRU Report No. 37, Bethesda, MD, 1984 (unpublished).
[17] Stopping power and range tables for electrons. Available from ⟨http://physics.nist.gov/PhysRefdata/Star/Text/STAR.html⟩.
[18] J. C. Oller, A. Muñoz, J. M. Pérez, F. Blanco, P. Limão-Vieira, and G. García, Chem. Phys. Lett. **421**, 439 (2006).
[19] A. Muñoz, J. C. Oller, F. Blanco, J. D. Gorfinkiel, and G. García, Chem. Phys. Lett. **433**, 253 (2007).
[20] A. Williart, P. A. Kendall, F. Blanco, P. Tegeder, G. García, and N. J. Mason, Chem. Phys. Lett. **375**, 39 (2003).
[21] P. Limão-Vieira, F. Blanco, J. C. Oller, A. Muñoz, J. M. Pérez, M. Vinodkumar, G. García, and N. J. Mason, Phys. Rev. A **71**, 032720 (2005).
[22] H. C. Straub, P. Renault, B. G. Lindsay, K. A. Smith, and R. F. Stebbings, Phys. Rev. A **54**, 2146 (1996).
[23] B. L. Schraam, F. J. de Heer, M. J. Van der Wiel, and J. Kistemaker, Physica (Amsterdam) **31**, 94 (1965).
[24] D. Rapp and P. Englander-Golden, J. Chem. Phys. **43**, 1464 (1965).
[25] R. R. Goruganthu, W. G. Wilson, and R. A. Bonham, Phys. Rev. A **35**, 540 (1987).
[26] C. B. Opal, E. C. Beaty, and W. K. Peterson, At. Data **4**, 209 (1972).
[27] A. Jain, J. Phys. B **21**, 905 (1988).
[28] G. Seng and F. Linder, J. Phys. B **9**, 2539 (1976).
[29] O. Sueoka, S. Mori, and Y. Katayama, J. Phys. B **19**, L373 (1986).
[30] C. Szmytkowski, Chem. Phys. Lett. **136**, 363 (1987).
[31] A. Zecca, G. Karwasz, S. Oss, R. Grisenti, and R. S. Brusa, J. Phys. B **20**, L133 (1987).
[32] H. Nishimura and K. Yano, J. Phys. Soc. Jpn. **57**, 1951 (1988).
[33] Z. Saglam and N. Aktekin, J. Phys. B **23**, 1529 (1990).
[34] Z. Saglam and N. Aktekin, J. Phys. B **24**, 3491 (1991).
[35] M. Kimura, O. Sueoka, A. Hamada, and Y. Itikawa, Adv. Chem. Phys. **111**, 537 (2000).
[36] R. Čurík, J. P. Ziesel, N. C. Jones, T. A. Field, and D. Field, Phys. Rev. Lett. **97**, 123202 (2006) and (private communication).
[37] G. García and F. Blanco, Phys. Rev. A **62**, 044702 (2000).
[38] F. Manero, F. Blanco, and G. García, Phys. Rev. A **66**, 032713 (2002).
[39] G. García, J. L. de Pablos, F. Blanco, and A. Williart, J. Phys. B **35**, 4657 (2002).
[40] M. Vinodkumar, K. N. Joshipura, C. Limbachiya, and N. Mason, Phys. Rev. A **74**, 022721 (2006).
[41] A. Faure, J. D. Gorfinkiel, and J. Tennyson, J. Phys. B **37**, 801 (2004).
[42] M. Inokuti and M. R. C. McDowell, J. Phys. B **7**, 2382 (1974).
[43] M. Inokuti, Rev. Mod. Phys. **43**, 297 (1971).
[44] M. Inokuty, R. P. Saxon, and J. L. Dehmer, Int. J. Radiat. Phys. Chem. **7**, 109 (1975).
[45] C. Champion, Phys. Med. Biol. **48**, 2147 (2003).
[46] C. Champion, H. Hanssen, and P.-A. Hervieux, J. Chem. Phys. **121**, 9423 (2004).
[47] S. Uehara, H. Nikjoo, and D. Goodhead, Phys. Med. Biol. **38**, 1841 (1993).
[48] D. Emfietzoglou, G. Papamichael, and M. Moscovitch, J. Phys. D **33**, 932 (2000).
[49] D. Emfietzoglou, K. Karava, G. Papamichael, and M. Moscovitch, Radiat. Prot. Dosim. **110**, 871 (2004).
[50] D. Emfietzoglou, F. A. Cucinotta, and H. Nikjoo, Radiat. Res. **164**, 202 (2005).
[51] D. Emfietzoglou and H. Nikjoo, Radiat. Res. **167**, 110 (2007).